JOURNAL OF NEUROTRAUMA 37:2277–2291 (November 1, 2020)

DOI: 10.1089/neu.2020.7050

Treadmill-Based Gait Kinematics in the Yucatan Mini Pig

Maxwell Boakye,[1] Johnny Morehouse,[1] Jay Ethridge,[1] Darlene A. Burke,[1] Nicolas K. Khattar,[1] Chitra Kumar,[1] Neda Manouchehri,[4] Femke Streijger,[4] Robert Reed,[1] David S.K. Magnuson,[1] Leslie Sherwood,[3] Brian K. Kwon,[4,5] and Dena R. Howland[1,2]

Abstract

Yucatan miniature pigs (YMPs) are similar to humans in spinal cord size as well as physiological and neuroanatomical features, making them a useful model for human spinal cord injury. However, little is known regarding pig gait kinematics, especially on a treadmill. In this study, 12 healthy YMPs were assessed during bipedal and/or quadrupedal stepping on a treadmill at six speeds (1.0, 1.5, 2.0, 2.5, 3.0, and 3.5 km/h). Kinematic parameters, including limb coordination and proximal and distal limb angles, were measured. Findings indicate that YMPs use a lateral sequence footfall pattern across all speeds. Stride and stance durations decreased with increasing speed whereas swing duration showed no significant change. Across all speeds assessed, no significant differences were noted between hindlimb stepping parameters for bipedal or quadrupedal gait with the exception of distal limb angular kinematics. Specifically, significant differences were observed between locomotor tasks during maximum flexion (quadrupedal > bipedal), total excursion (bipedal > quadrupedal), and the phase relationship between the timing of maximum extension between the right and left hindlimbs (bipedal > quadrupedal). Speed also impacted maximum flexion and right-left phase relationships given that significant differences were found between the fastest speed (3.5 km/h) relative to each of the other speeds. This study establishes a methodology for bipedal and quadrupedal treadmill-based kinematic testing in healthy YMPs. The treadmill approach used was effective in recruiting primarily the spinal circuitry responsible for the basic stepping patterns as has been shown in cats. We recommend 2.5 km/h (0.7 m/sec) as a target walking gait for pre-clinical studies using YMPs, which is similar to that used in cats.

Keywords: kinematics; large animal model; porcine model; spinal cord injury; treadmill

Introduction

Spinal cord injury (SCI) currently affects >17,000 people in the United States each year.[1] Despite many therapeutic approaches showing promise in rodents, there are currently no convincing efficacious pharmacological treatments for acute and chronic human SCI.[2–4] Significant anatomical, functional, molecular, and pathological differences between the rodent and human spinal cords have been cited as possible reasons for failure to translate rodent trial results to human clinical practice.[5–10] As a result of these limitations, there is rising interest in the use of large mammalian species as intermediary models of SCI to facilitate research translation for human SCI.[11] In addition to the cat, canine, and ovine larger animal models of SCI, [2–22] a Yucatan miniature pig model was recently described.[23] This pig model has several features that may have translational relevance, including spinal cord size, a greater cerebrospinal fluid (CSF) to spinal cord ratio, and some physiological and neuroanatomical similarities to the human spinal cord.[23–28] The larger spinal canal and cord of the pig allows for testing of emerging spinal neuromodulating therapies, like epidural stimulation, using surgical techniques and neuromodulatory devices similarly sized to those used in humans.[29–32] However, because of its relatively recent introduction to SCI research, very little is known regarding the kinematics of the pig and how these animals walk on a treadmill.

The Porcine Thoracic Injury Behavioral Scale (PTIBS) has been used to evaluate behavioral outcomes after SCI[23] and is the most common scale used to evaluate overground locomotor outcomes in porcine SCI, pre-clinical studies.[26,33–35] The PTIBS is similar to the Basso, Beattie and Bresnahan (BBB) scale used to assess locomotion in rats, in that they are both based on visual inspection.[36] Unlike the BBB, which has been combined extensively with kinematic studies to evaluate SCI outcomes in rodents, the sensitivity of the PTIBS to subtle changes and its correlation with more

[1]Department of Neurological Surgery and Kentucky Spinal Cord Injury Research Center, [3]Research Resources Facilities, University of Louisville, Louisville, Kentucky, USA.
[2]Research Service, Robley Rex Veterans Affairs Medical Center, Louisville, Kentucky, USA.
[4]International Collaboration on Repair Discoveries, [5]Vancouver Spine Surgery Institute, Department of Orthopedics, University of British Columbia (UBC), Vancouver, British Columbia, Canada.

standardized kinematic measures remains untested. In both rodents and more recently in larger animals, treadmill-based kinematic parameters have proven valuable for detection of more subtle, as well as different, improvements brought about by therapeutic interventions.[37–43] There are multiple advantages to the use of the treadmill. In particular, the placement of weight-support systems is simpler than in an open-field arena, speeds can be tightly controlled, and circuitry mediating hindlimb versus forelimb stepping tested through bipedal and quadrupedal stepping tasks.[44]

In experimental animal and clinical SCI studies, kinematic and gait measures depicted as cyclograms have proven valuable adjuncts by providing a fuller understanding of both temporal and spatial changes in stepping after SCI. In fact, they have been proposed as a measure of SCI that may be used to stratify patients for clinical trials.[45–52] Although several studies have evaluated overground porcine gait kinematics,[53–55] we found only one study that addressed limb kinematics of the Yucatan miniature pig (YMP) on the treadmill. Our study extends those initial, but relatively limited, findings by assessing multiple walking speeds, two gait tasks, and a larger number of gait-related kinematic parameters.

The large body of treadmill-based kinematic studies performed in the cat since the early 1930s provides a roadmap for similar studies in the pig.[13–22,56–76] The aim of this study was to characterize treadmill-based kinematics of healthy YMPs in anticipation of future comparisons in animals with SCIs. As has been done in many rodent and feline studies to establish normal performance features, we evaluated the effects of treadmill speed on kinematic parameters and limb coordination.[18,21,38,56,64] Additionally, as in earlier studies, we also compared bipedal to quadrupedal kinematics.[77–82] The overall intent is to add treadmill-based kinematics to the PTIBS in the evaluation of locomotor outcomes in the YMP model of SCI.

Methods

The animals used for this study ($n = 12$) were 6-month-old female YMPs with weights of 20–30 kg, purchased from Sinclair BioResources (Auxvasse, Missouri). Females were used because of ease of bladder catherization and care relative to males in anticipation of their use in SCI studies. This study was approved by the University of Louisville (UofL) Institutional Animal Care and Use Committee and conducted in accordance with the *Guide for the Care and Use of Laboratory Animals*, 8th edition.[42] The UofL animal care program is accredited by the Association for the Assessment and Accreditation of Laboratory Animal Care International. Environmental housing conditions were 72°F (22.2°C), 30–70% humidity, with 10–15 fresh air changes per hour, and a 12:12-h light/dark cycle. Animals were housed socially in floor pens with 5–10 cm of Cellu-nest™ bedding (Shepherd Specialty Papers, Watertown, TN) on top of 0.95-cm-thick 1.22 × 1.22 m interlocking Rubber Gym Tiles (Rubber Flooring Inc., Mesa, AZ) and provided with environmental enrichment, including toys and videos. Pigs were fed a standard laboratory mini-pig grower diet (5081; LabDiet, St. Louis, MO) and received filtered tap water.

Upon arrival, pigs were acclimated for 7 days (not including the day of arrival). During this period, the trainer spent 15 min per day in the animal's pen. This period each day allowed pigs to become acclimated to the trainer, which included hand feeding a portion of their ration the last 2 days of acclimation.

Training

Once the animals were released from quarantine, they began positive reinforcement training or clicker training.[83–86] Training consisted of three to four 10- to 20-min sessions for a maximum of 1 h per day for 3 weeks. All animals acclimated well to training. Each was trained to complete multiple tasks and achieve the end goal of walking in a straight line on the treadmill (PetRun PR720E modified with a clear 0.32-cm-thick polycarbonate panel in the front that has an 8.89-cm target centered with adjustable heights) while holding their snout against a target (Table 1). First, using a SunGrow dog clicker (Luffy Pets Collection, Traverse City, MI), the pigs were conditioned to recognize that a click meant they would receive a reward (daily food rations were used as the reward). This pairing conditioned the click as the reinforcement for the desired behaviors. Next, they were trained to recognize a given name so the trainer could get their attention on cue. After that, animals were trained to touch and hold their snouts to a Karen Pryor buoy target (Karen Pryor Clicker Training, Watham, MA) for up to 1 min as well as follow the target while walking.

Pigs were then acclimated to the sound of the treadmill and the movement of the belt. Once acclimated to the treadmill, the animals were trained to walk while holding their snouts against the target mounted on the front of the treadmill. Rewards were delivered through an opening in the panel, located just above the target. Their behavior was then shaped to step in the center of the treadmill while keeping their body straight for up to 1 min (30–60 contiguous steps). Next, a platform was placed across the treadmill and the animals were conditioned to stand with their forelimbs on the platform while performing bipedal stepping with their hindlimbs. Filming took place once the pigs could perform each task consistently. Typically, it took 45 min to an hour per day for 2 weeks for a pig's performance to be consistent.

Filming

The day before filming, while pigs were standing and holding their snout on a target, a red Sharpie® was used to mark the skin overlying the tuber coxae (C), greater trochanter (G), tibiotarsal joint (T), and metatarsophalangeal joint (M) of each hindlimb. On the day of filming, 0.95-cm-diameter, spherical, reflective markers were placed over the eight Sharpie® marks placed the day before (Fig. 1). Spherical markers were used because they tracked more consistently in these positions. Additionally, 1.27-cm-diameter reflective markers were placed on each hoof with one edge of the marker touching the coronary band and another edge touching the ventral aspect of the wall of the hoof.

Pigs were filmed as they stepped on the treadmill for trials of up to 1 min. Three GoPro Hero 3+ Silver cameras were used to film the animals, and they were triggered simultaneously with a GoPro remote (GoPro, San Mateo, CA; Fig. 2). Two of the cameras were positioned 73 cm perpendicularly from the lateral edges of the treadmill and focused on the walking area for the hindlimbs. The third camera was placed 89 cm perpendicularly from the back edge of the treadmill centered with the middle of the belt. The video was recorded with a resolution of 720 p at 120 frames per second (120 Hz). Animals were filmed at six speeds performing bipedal and quadrupedal stepping. The six speeds utilized were 1.0, 1.5, 2.0, 2.5, 3.0, and 3.5 km/h (0.3, 0.4, 0.6, 0.7, 0.8, and 1.0 m/s). Speeds were determined by the available settings on the treadmill and were the lowest six settings. The speeds utilized also encompass the normal walking velocity of a YMP.[35] During filming, the goal was ≥10 steps on each task at each speed while walking in a straight line with snout on the target. A minimum of three attempts at each speed for each task were captured.

Once the videos were collected, 10 contiguous step cycles that best represented the animal's typical stepping behavior were selected. Each step cycle (stride) started with the initial contact of the hoof with the treadmill, followed by the stance phase that ended at the hoof lifting from the treadmill, and a swing phase ending the frame before the next initiation of contact. The determined step cycles were then digitized using MaxTRAQ 2D software (Innovision Systems, Marietta, GA). The stance phase was determined by

Table 1. Tasks or Behaviors in Sequential Order and the Shaping for Each Task

‘‘Charging the Clicker’’	1. During first training session, allow the animals to acclimate to the training room until they appear comfortable. 2. Click the clicker and immediately reward the animal. The goal is for the pig to understand that click means reward. 3. After clicking and rewarding (C&R) the animal several times, start having the animal look for or move to get the reward instead of immediately presenting the reward after the click. 4. Next, allow the pig’s attention to be focused on something other than the trainer and then click the animal. Once the pig immediately turns and looks for the treat, when clicked the clicker is charged.
Name Cue	1. Get the pig to look up at you and then C&R. Trainer can accomplish this by using his or her hand to get the animal’s attention and then bringing it up toward his or her face. 2. After the trainer can repeatedly get the animal to look up at him or her, say the pig’s designated name que while it’s looking up and then C&R. 3. Once the pig regularly looks up at the trainer when its name is said, allow the pig to wander away or have its attention elsewhere and then give name cue. When the animal responds to the name by looking up or turning around, immediately C&R. 4. Finally, the trainer needs to allow the animal to walk away or walk away from the animal and say its name. When the animal starts walking back toward the trainer, he or she should C&R. Continue with several repetitions until behavior is instant and consistent.
Target Training	1. Present target, and when pig touches target with snout, C&R. 2. Once animal touches target, as soon as target is presented add the cue ‘‘Touch.’’ 3. Name cue can be added as well ‘‘Name of animal and touch.’’ 4. Repeat until animal touches target instantly and consistently on cue.
Hold the Target	1. Give touch cue and allow the pig to touch the target with its snout for at least 2 sec, then C&R. 2. Continue giving touch cue while having the animal touch the target with its snout for longer periods of time before C&R. 3. Once the pig holds the target for 5–10 sec, only click and treat when it is standing completely still. 4. When the pig holds the target while remaining still for 5 sec, add ‘‘Stay’’ cue. Say touch and when the pig touches, say ‘‘Stay.’’ Only C&R when the animal holds completely still while touching the target. 5. Repeat touch and stay cue and continually have the animal stay for longer periods of time before C&R (minimum of 15 sec before moving on).
Walk Cue	1. Give touch cue with target at your side, then stay cue when animal touches target. Walk away with target at your side, and if the animal follows it, C&R. 2. Repeat several times having the pig walk further each time before C&R. (Do not C&R if pig is rooting at target.) 3. Once the pig walks the length of the training room following the target without rooting at it, add ‘‘Walk’’ cue after ‘‘Stay’’ cue and before you take off walking.
Treadmill	1. Have the animal touch the target and stay lined up so it can walk up onto the treadmill. Give walk cue and lead the pig up on the treadmill. C&R when animal steps onto the treadmill. 2. After the pig gets on and off of the treadmill without hesitation, have it touch target on the front panel of the treadmill, then C&R. 3. Train the animal to hold the target on the treadmill the same way you trained it to hold target using the cue ‘‘Hold’’ instead of stay. 4. Acclimate the animal to the treadmill by turning the treadmill on and walking the pig around the treadmill following the target while C&R until it appears comfortable. 5. Once it is comfortable with treadmill running, have the pig touch and hold the target while the treadmill is off. Turn the treadmill on and give walk cue. If the animal takes a step or two, click and treat while turning the treadmill back off. If the animal does not take a step, repeat the process until it does and then C&R. Do not allow the pig to fall off the treadmill if it is not stepping right away. Shape the pig’s behavior to walk straight in the middle of the treadmill while holding the target without rooting at it for at least 10 contiguous steps.

The tasks are trained in the order found to have the most success, and it is important not to move to the next task until the animal has learned the previous one.

digitizing each hoof marker starting with initial contact on the treadmill through hoof lift off. The swing phase was the time that was not digitized until initiation of the next initial contact. Twelve parallel lines were marked on the treadmill belt (numbered 1–12 starting from the right; Fig. 2). Each line was calibrated based upon its distance from the right lateral camera.

Video capture with a meter stick marked at 30 cm on each line of the treadmill gave us a pixel per 30-cm conversion for each line. This improves the accuracy of spatial measurements, such as stride and stance distances, given that the step may not always be at a consistent (same) distance from the camera every time. Videos were digitized in MaxTRAQ, and a conversion ratio for pixels to centimeters was calculated for each line. Conversion ratios were checked for accuracy by two perpendicular lines on the treadmill belt that were 30 cm apart. These lines also were digitized in MaxTRAQ and, using the conversion tool in the software, were compared with the predetermined conversion ratio. The 10 step cycles chosen for analyses were viewed using the caudal camera, and an average line of calibration was selected. If the hoof fell between two lines, the average of the selected lines was calculated and that value used for the calibration of that limb. For intralimb analysis, the four spherical markers were digitized using the same 10 step cycles that were digitized using the hoof markers.

Statistical analysis

Each file was saved as a MaxTRAQ ASCII file and then processed through a custom Visual Basic for Applications (VBA)

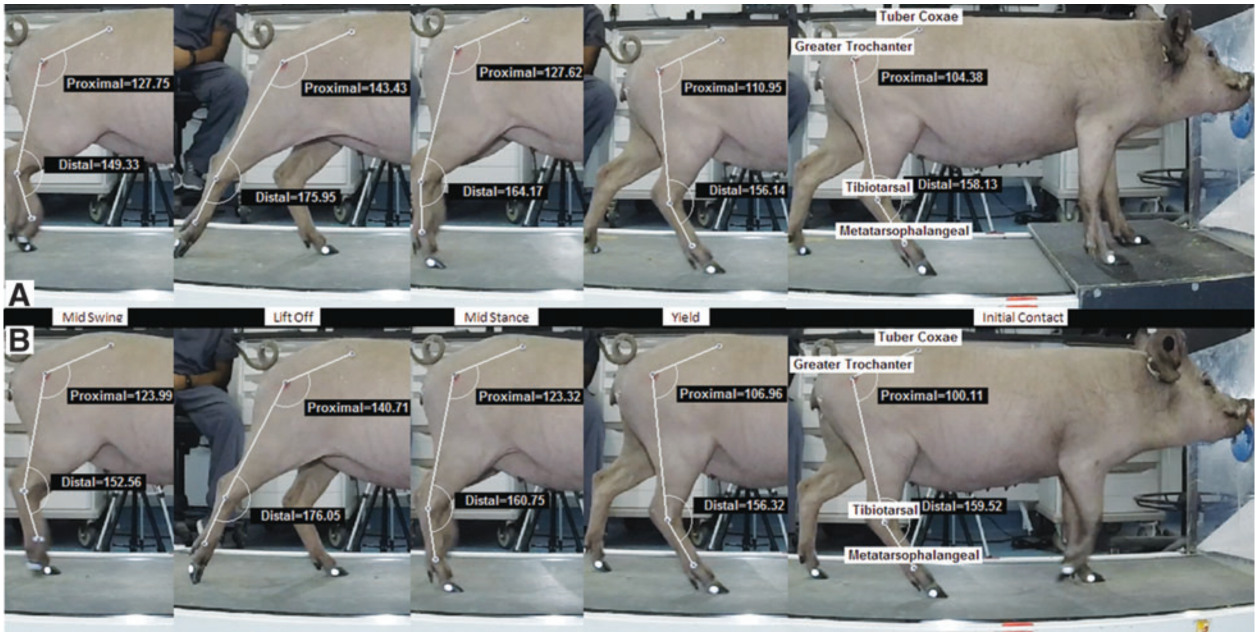

FIG. 1. Images of the pig displaying (**A**) bipedal and (**B**) quadrupedal treadmill stepping during key stepping landmarks. Proximal and distal angles are labeled to show changes in the angles at these landmarks. Demonstrated by moving right to left: initial contact, yield, mid stance, lift off, and mid swing.

Excel add-in. The ASCII file contained the location in XY coordinates and the frame numbers of all markers through the trial. This add-in calculated multiple parameters (Table 2), as well as extracting the exact frames of initial contact and lift off. Kinematic outcome measures of quadrupedal forelimb stepping at multiple speeds were analyzed using repeated-measures (RM) analysis of variance (ANOVA). Significant differences among speeds were compared using Bonferroni's post-hoc *t*-tests for multiple comparisons. Analyses of bipedal and quadrupedal stepping at each speed were analyzed using RM ANOVA followed by Bonferroni's post-hoc *t*-tests. Comparison of two- or four-limbs differences (2 = hindlimbs only or 4 = fore- and hindlimbs) and differences among speeds (1.0, 1.5, 2.0, 2.5, 3.0, and 3.5 km/h) were analyzed using RM ANOVA followed by Bonferroni's post-hoc *t*-tests. (IBM SPSS v25; IBM Corp., Armonk, NY).

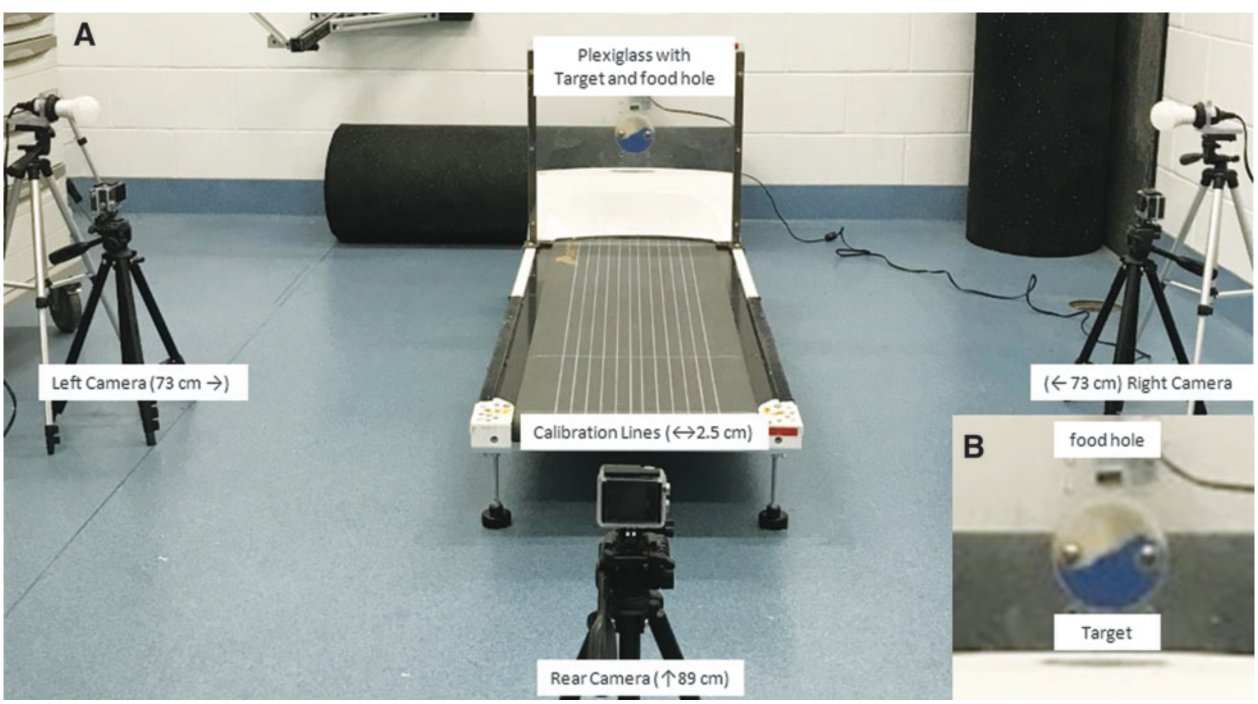

FIG. 2. Image showing (**A**) the location of the cameras and lights in respect to the treadmill. (**B**) The target and food hole used for training.

Table 2. Means and SD of Kinematic (Upper) and Coupling (Lower) Treadmill Stepping Measures during Bipedal and Quadrupedal Stepping in Intact Pigs at Six Speeds (km/h)

(km/h)	Bi (1.0) Mean	SD	Q (1.0) Mean	SD	Bi (1.5) Mean	SD	Q (1.5) Mean	SD	Bi (2.0) Mean	SD	Q (2.0) Mean	SD	Bi (2.5) Mean	SD	Q (2.5) Mean	SD	Bi (3.0) Mean	SD	Q (3.0) Mean	SD	Bi (3.5) Mean	SD	Q (3.5) Mean	SD
Stance time (s)	1.19	0.10	1.10	0.16	0.82	0.07	0.79	0.10	0.64	0.04	0.64	0.06	0.54	0.04	0.54	0.05	0.44	0.01	0.44	0.02	0.38	0.00	0.38	0.02
Stride time (s)	1.35	0.19	1.47	0.13	1.04	0.13	1.09	0.09	0.89	0.08	0.91	0.06	0.79	0.07	0.80	0.06	0.67	0.04	0.71	0.03	0.60	0.02	0.62	0.03
Stance length (cm)	29.65	4.07	31.06	2.77	31.89	4.37	31.43	2.15	33.65	2.70	32.19	2.00	34.37	2.36	33.22	1.72	33.96	1.02	33.11	0.51	33.97	0.56	33.42	0.59
Stride length (cm)	36.30	4.86	38.33	3.51	42.20	5.64	41.76	3.40	46.49	3.53	45.60	3.12	49.90	3.48	49.32	3.77	51.19	2.77	52.80	3.23	52.91	2.18	54.88	4.03
Average speed (cm/s)	26.99	0.47	26.13	0.73	40.50	1.59	38.49	1.50	52.57	1.46	50.12	0.73	63.36	2.65	61.72	2.81	76.79	0.94	74.64	1.78	88.57	3.28	87.96	2.66
Overall speed (cm/s)	26.99	0.47	26.13	0.73	40.50	1.58	38.49	1.50	52.57	1.46	50.12	0.72	63.36	2.65	61.71	2.81	76.79	0.94	74.64	1.77	88.57	3.28	87.95	2.65
Pct swing	18.38	1.56	18.95	2.11	24.45	1.47	24.62	3.12	27.64	1.42	29.34	2.56	31.10	1.63	32.43	3.63	33.55	2.86	37.14	3.58	35.74	2.35	38.91	3.60
Pct stance	81.62	1.56	81.05	2.11	75.55	1.47	75.38	3.12	72.36	1.42	70.66	2.56	68.90	1.63	67.57	3.63	66.45	2.86	62.86	3.58	64.26	2.35	61.09	3.60
Angle 1																								
Peak (deg)	184.90	3.25	180.89	3.31	183.92	4.06	180.27	3.14	182.60	3.38	179.06	3.10	183.01	4.27	180.07	3.44	181.43	5.62	180.11	2.90	180.13	5.52	179.67	2.58
Trough (deg)	147.93	4.95	158.11	3.99	148.66	3.75	157.41	4.10	148.20	3.16	154.50	3.91	148.13	3.16	153.93	3.63	147.39	1.42	150.06	2.32	146.33	2.05	148.97	2.55
Excursion (deg)	36.97	5.21	22.78	4.15	35.26	4.18	22.86	3.78	34.40	3.80	24.56	2.99	34.88	4.24	26.15	3.47	34.04	6.10	30.05	3.95	33.80	6.30	30.69	2.56
Angle 2																								
Peak (deg)	142.88	4.67	137.60	5.47	142.47	4.78	138.85	4.40	143.29	4.23	140.09	3.91	143.62	3.59	141.11	3.97	143.75	3.25	141.34	2.62	144.39	3.10	139.71	2.30
Trough (deg)	106.06	3.60	104.17	6.08	105.50	4.51	101.85	5.64	104.42	3.77	100.21	4.23	103.16	4.57	99.10	4.93	102.85	4.83	98.53	2.96	104.06	5.82	96.54	2.74
Excursion (deg)	36.83	3.04	33.42	3.17	36.97	2.96	37.00	3.52	38.87	2.98	39.88	2.50	40.45	3.47	42.01	2.26	40.90	3.23	42.81	0.65	40.32	3.86	43.17	1.73
Phase 1 and 2	0.94	0.02	0.95	0.03	0.95	0.01	0.92	0.04	0.95	0.02	0.91	0.02	0.96	0.02	0.93	0.02	0.97	0.01	0.94	0.02	0.97	0.01	0.96	0.01
FRRL			0.317	0.057			0.285	0.038			0.272	0.023			0.266	0.025			0.276	0.023			0.276	0.010
FRFL			0.514	0.017			0.498	0.018			0.505	0.012			0.502	0.009			0.502	0.004			0.500	0.003
FRRR			0.793	0.035			0.780	0.024			0.768	0.024			0.764	0.020			0.769	0.018			0.771	0.011
FLRL			0.804	0.044			0.785	0.039			0.768	0.024			0.765	0.027			0.775	0.023			0.777	0.009
FLFR			0.487	0.016			0.501	0.017			0.495	0.012			0.498	0.008			0.497	0.005			0.500	0.003
FLRR			0.280	0.030			0.282	0.030			0.263	0.024			0.262	0.022			0.267	0.018			0.271	0.010
RRFR			0.205	0.037			0.219	0.024			0.232	0.024			0.237	0.019			0.231	0.018			0.230	0.011
RRRL	0.520	0.028	0.500	0.030	0.503	0.015	0.503	0.020	0.505	0.008	0.501	0.015	0.503	0.010	0.503	0.009	0.507	0.007	0.506	0.012	0.505	0.009	0.509	0.002
RRFL			0.718	0.031			0.718	0.027			0.737	0.024			0.738	0.022			0.733	0.017			0.730	0.010
RLFL			0.197	0.046			0.213	0.040			0.232	0.024			0.236	0.026			0.225	0.023			0.223	0.010
RLRR	0.476	0.029	0.499	0.031	0.495	0.016	0.496	0.018	0.496	0.008	0.498	0.016	0.497	0.010	0.497	0.009	0.492	0.008	0.493	0.013	0.495	0.009	0.491	0.003
RLFR			0.683	0.054			0.715	0.038			0.728	0.022			0.734	0.026			0.723	0.024			0.723	0.010

Treadmill kinematic stepping measures are listed for selected stance, swing, stride, and speed outcome measures (top). The lower portion shows hindlimb and forelimb coupling measures of coordination (e.g., FRRL [Front Right Rear Left]), homologous (e.g., FRFL [Front Right Front Left]), and homolateral (e.g., FRRR [Front Right Rear Right]) side measures at six speeds in km/h.

Pct, percent; SD, standard deviation.

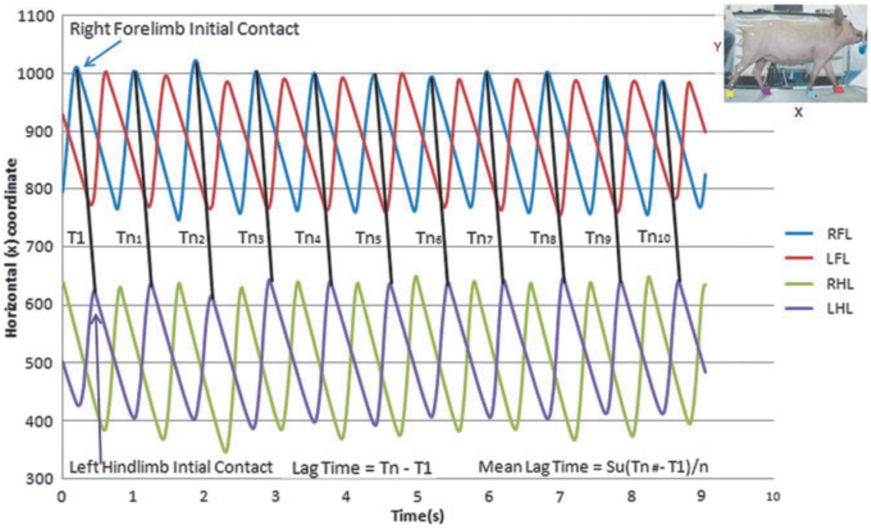

FIG. 3. Multiple stepping patterns over time can be illustrated using sine waves of alternating stance and swing cycles (top). Peaks of the waves represent the moment of maximum forward movement. Lines connecting the peaks of the forelimb with its diagonal hindlimb show the time lapses between the diagonal limbs. Mean lag time is calculated by taking the average of the sum of the subsequent lag times subtracted from the first lag time.

In addition, interlimb coordination was assessed by utilizing gait diagrams of the left forelimb (LF), right forelimb (RF), left hindlimb (LH), and right hindlimb (RH) and determination of homologous (LF, RF, LH, and RH), homolateral (LF, LH, RF, and RH), and diagonal (LF, RH, RF, and LH) coupling patterns.[87,88] Coupling measures were calculated as a percentage of the step cycle using the methods previously described in LeBlond and colleagues and also depicted using polar plots to assess the distribution and variability at different speeds.[28,39,62] The mean diagonal coupling interval, a measure of the coordination between the diagonal limbs, also was calculated using the list of the horizontal (x) coordinates of the markers on each hoof as follows: Mean diagonal coupling interval = Tn – T1/number of steps; Tn is the interval between the ''nth'' right hindlimb and ''nth'' left forelimb placement, T1 is the interval between the first right hindlimb and first left forelimb hoof placements[40] and was plotted as a function of step number (n; Fig. 3). Mean diagonal coupling intervals remain virtually zero in normal animals, but once an animal experiences a disruption in their locomotor capabilities, the time interval grows with each step.

Traditional intralimb kinematic assessments in other animal species include the knee.[40,69,88–90] However, because of the extensive movement of the knee under the skin in many species, including mini pigs, accurate identification of the knee relies on triangulation using the known positions of the hip and ankle, and the known lengths of the femur and tibia. This process can be labor intensive or require expensive software packages. We therefore used a two-dimensional (2D) approach previously used for rats to quantify changes in intralimb kinematics after SCI simply and effectively.[89,91] This approach uses markers on the anterior rim of the pelvis (I), head of the greater trochanter (H), lateral malleolus of the ankle (A), and metatarsophalangeal joint of the toe (T) to create a three-segment (I-H, H-A, and A-T), two-angle (I-H-A and H-A-T) limb model that easily detects changes in limb movement.[86–88] The markers located at C, G, T, and M define three segments (C-G, G-T, and T-M; Fig. 1), a distal angle (G-T-M; Figs. 1 and 4A), and a proximal angle (C-G-T; Figs. 1 and 4B).

Using initial hoof contacts, determined visually from the digital recordings, each trial was divided into individual step cycles. From these step cycles the maximum (peak = maximum extension) and minimum (trough = maximum flexion) for each of the two hindlimb angles was determined. Range of motion across each joint (angular excursion) was calculated by subtracting the trough values from the peak values. In addition, the phase relationship between the two angles was calculated by using the ratio of the peak to peak times relative to the step cycle duration. The proximal angle describes the range of motion across the hip and knee, whereas the distal angle reflects the motion of the knee and ankle. Using this approach, subtle differences can be detected in the proximal and/or distal angles (Fig. 4A,B), changes in the maximal extension and flexion angles, and excursions of both proximal and distal limb angles, and changes in the shape and structure of the angle-angle plots (Fig. 4C). These figures also give us the opportunity to observe the extension and flexion intervals and how they can change. This method allows us to use an inexpensive camera/software combination to capture the animal in 2D, digitize each video in ~ 10 min, and (through a custom VBA Excel add-in) extract the data quickly, all resulting in a relatively high throughput.

Results

Step cycle parameters

Step cycle durations for each limb were obtained at multiple treadmill speeds in all 12 pigs. Figure 5 shows step cycle durations as a function of speeds ranging from 1.0 to 3.5 km/h. Average step cycle durations are summarized in Table 2. At a speed of 2.5 km/h, the average step cycle duration was 0.80 ± 0.069 sec with a percent stance (duty factor) of $68.9 \pm 3.01\%$. Stride (stance + swing) and stance durations decreased with increasing speed (stride: $F = 145$, $df = 5,19$, $p < 0.001$; stance: $F = 276$, $df = 5,15$, $p < 0.001$; Fig. 5A,C) whereas the swing duration showed no statistically significant change ($F = 1.7$, $df = 5,13$, $p > 0.05$; Figure 5B). For the forelimbs, significant differences in stance time ($F = 71.3$, $df = 5,9$, $p < 0.001$), stride time ($F = 64.4$, $df = 5,9$, $p < 0.001$), and percent stance and swing ($F = 55.3$, $df = 5,6$, $p < 0.001$) were observed between the two lowest speeds and all other speeds (1.0 vs. 1.5–3.5 km/h and 1.5 vs. 2.0–3.5 km/h). Step cycle parameters were stable with no differences between 2.0 and 2.5 km/h (all, $p > 0.05$); however, significant differences emerged between 2.0 and 2.5 km/h with 3.0 and 3.5 km/h (all comparisons: $p \leq 0.05$). There were no differences in stance distances between left and right hindlimbs at any speed

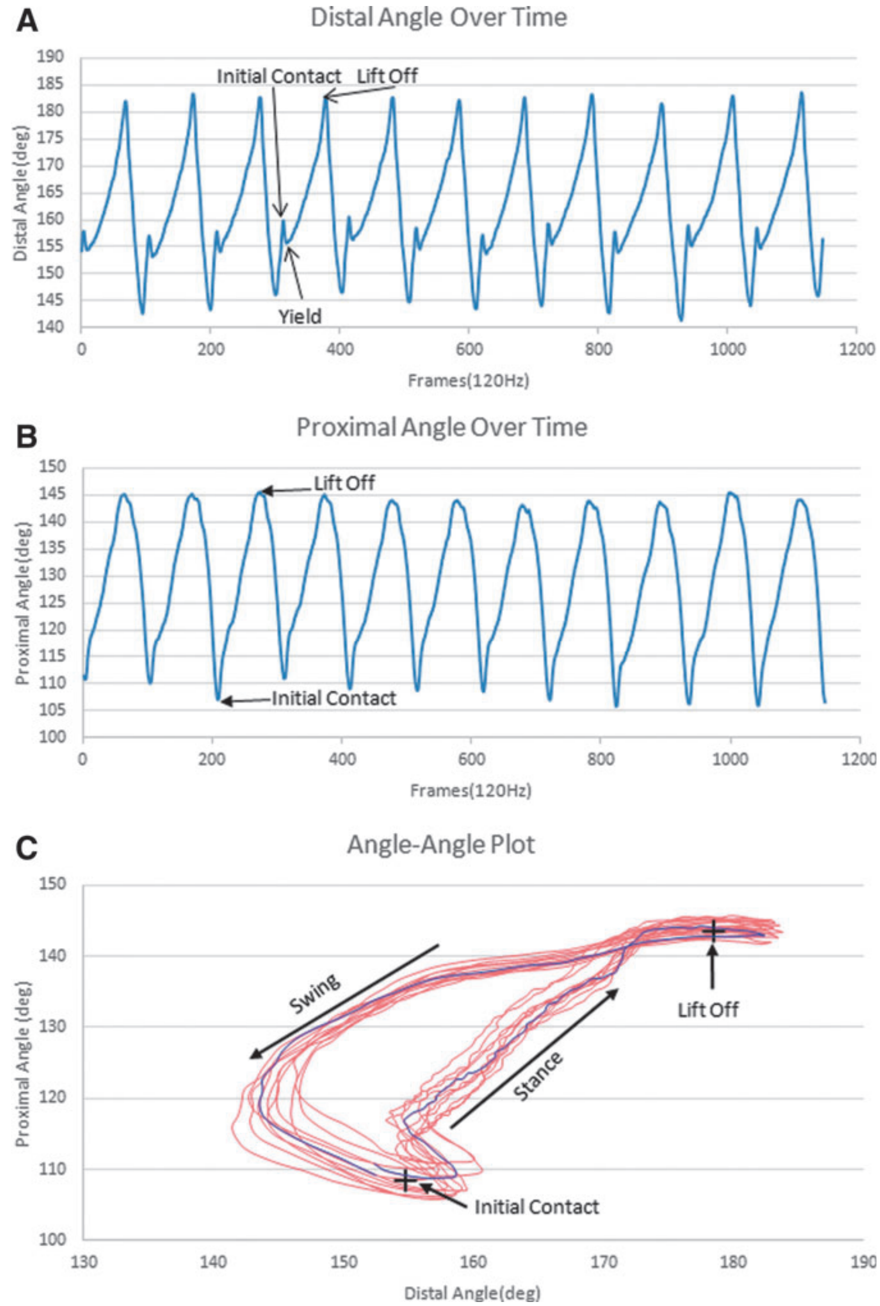

FIG. 4. Graphs of (**A**) distal angle, (**B**) proximal angle, and (**C**) proximal-distal angles during treadmill stepping showing the changes in the angles during movement during a period of 10 step cycles. (A) In a graph of the distal angle over time, the stepping landmarks of initial contact, yield, and lift off can be identified. (B) Similar to the distal angle over time, the initial contact and lift off are identifiable in the proximal angle over time. (C) When the angles are plotted against one another, you can see a distinctive shape and change in angle relationship between stance and swing. The red lines are the plots of 10 consecutive step cycles, with the blue line showing a typical single step cycle.

tested (all speeds, $p > 0.05$). Significant differences in stride distances were observed between 1.5 and 2.0 km/h with 3.5 km/h (both, $p \leq 0.05$).

For both bipedal and quadrupedal stepping, stance time, stride time, percent stance, and percent swing of the hindlimbs varied significantly with speed ($p \leq 0.0.05$), with the exception of stride duration during quadrupedal stepping between 2.0 and 2.5 km/h ($p = 0.076$). There were significant differences in stride distance between 1.0 km/h and all speeds, as well as between 1.5 and 2.0 and 3.5 km/h (all, $p \leq 0.05$). Similar to the forelimbs, there were no speed-related significant differences in swing duration ($F = 1.7$, $df = 5{,}13$, $p > 0.05$) and stance distance ($F = 4.1$, $df = 5{,}19$, $p = .012$), but there were no significant post-hoc comparisons. At each speed, there were no significant differences between bipedal and quadrupedal hindlimb stepping parameters (all, $p > 0.05$).

Importantly, this shows that the testing was sensitive enough to show differences between speeds in the speed related measures. Second, it also shows that the speeds from 2.0 to 3.0 km/h were the least variable in the non-speed-related measures. Third, it depicts the lack of differences in these kinematic stepping parameters

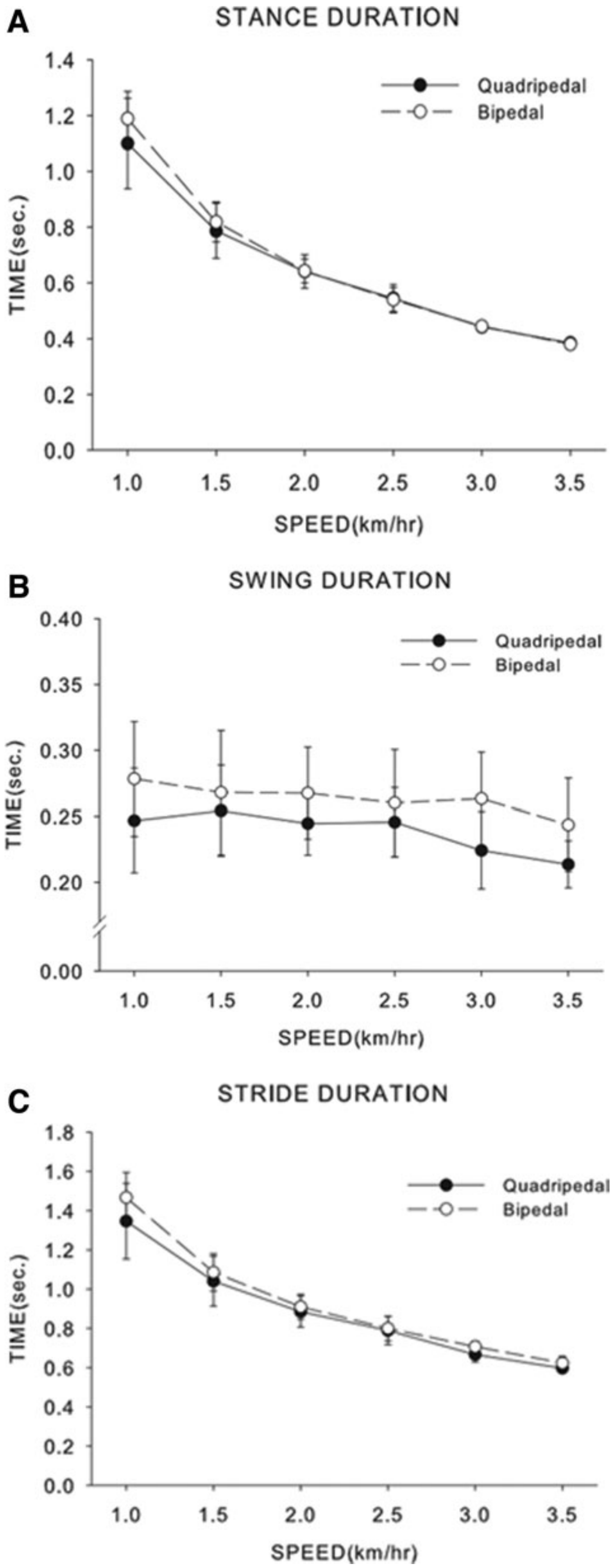

FIG. 5. Kinematic outcome measures of the (**A**) stance, (**B**) swing, and (**C**) stride duration during treadmill stepping comparing changes in speed. Quadrupedal and bipedal duration means and standard deviations illustrate that there is no influence of speed on the duration of swing either quadrupedal or bipedal while both stance and stride time steadily decrease in both quadrupedal and bipedal stepping as speed increases.

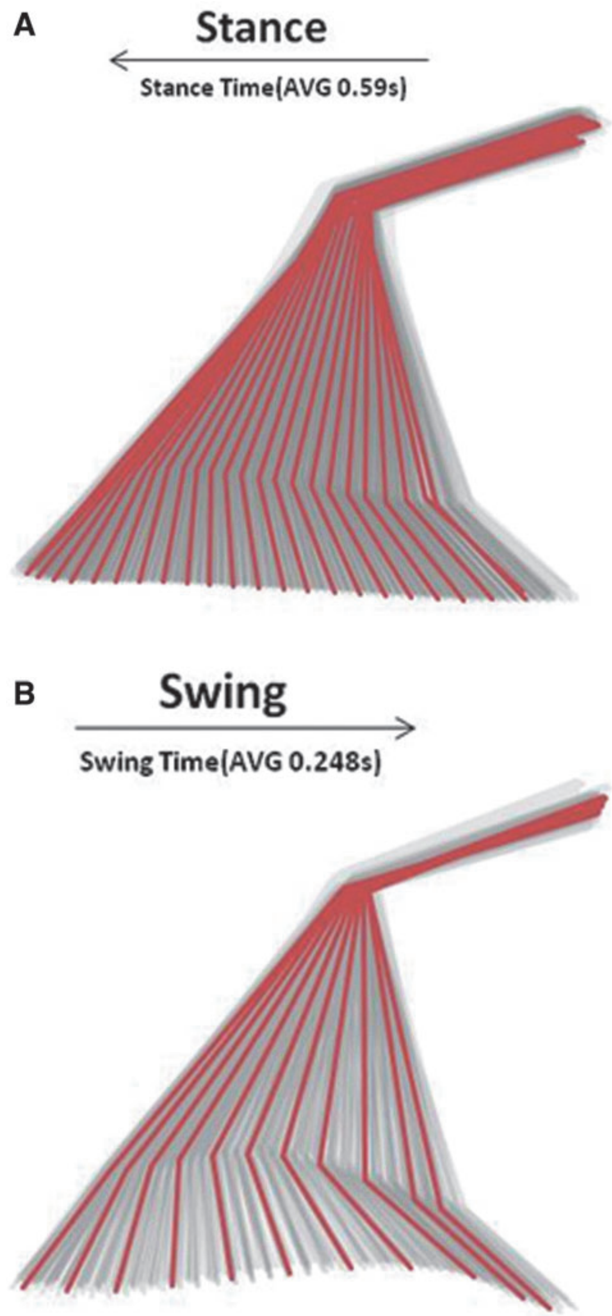

FIG. 6. Kinematic analysis of treadmill stepping is shown for a representative normal uninjured animal at 2.5 km/h. Example shown was taken from the right limb of an animal walking bipedally. Stick figure diagrams of the stance (**A**) and swing (**B**) cycles of one step cycle at 15 Hz (darker lines) and 10 step cycles at 120 Hz (lighter color) during stepping illustrate the movement across the hip and ankle.

between bipedal and quadrupedal stepping in the normal YMP. Collectively, these findings suggest that comparison across similarly sized YMPs at the same treadmill speed to a common (normative) baseline measure may be reasonable if an animal does not complete a stepping task (i.e., not tested) or data are lost or compromised during normative testing.

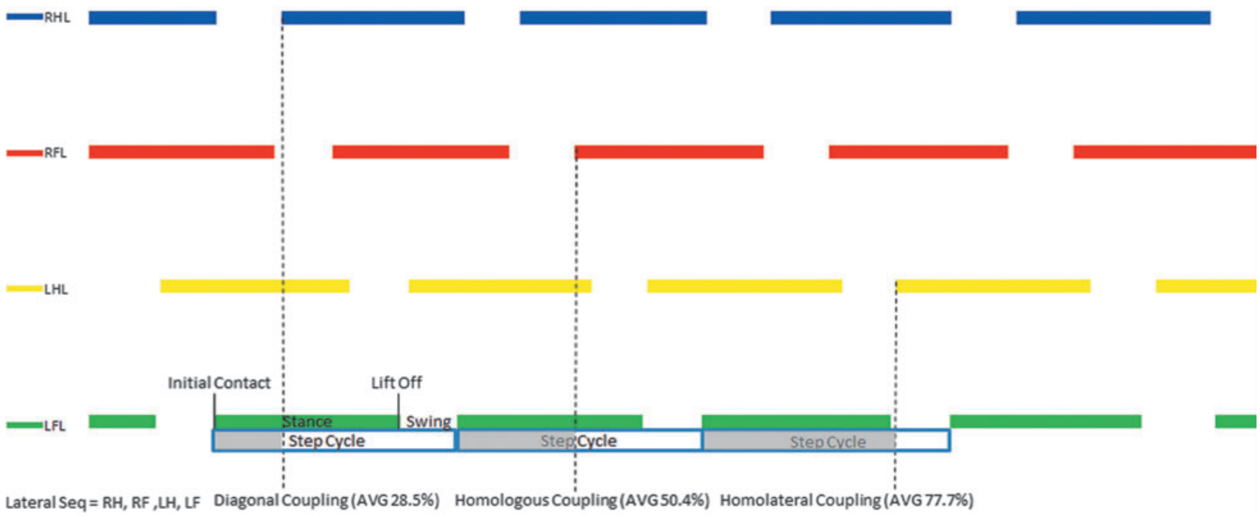

FIG. 7. A duty graph of quadrupedal stepping shows alternating patterns of the hindlimbs (LHL, RHL) and forelimbs (LFL, RFL) for the left and right sides (2.5 km/h). Diagonal coupling is shown by the initial contact of the right hindlimb (RHL) after the swing phase in relation to the cycle of the alternate left side forelimb (LFL) illustrated by the vertical dashed line. Homolateral right side steps are illustrated from the initial contact of the left side hindlimb (LHL) in relation with the cycle of the LFL (middle dashed line). Alternation of forelimbs is shown using the placement of the right-side forelimb (RFL) after the swing phase in relation to the cycle of the LFL (homologous) represented by the third dashed line. In addition to the other measure, by following the order of step initiation in the graph you can observe a lateral sequence of RHL, RFL, LHL, LFL.

Angular kinematics

Stick figure representations of the hindlimbs showed consistent patterns across multiple step cycles with little variability in the stance (Fig. 6A) and swing (Fig. 6B) phases. Figure 4 shows the distal (Fig. 4A) and proximal angles (Fig. 4B) for 10 step cycles. Distal and proximal angle-angle cyclograms also showed consistent angular movement patterns, reflecting consistent intralimb coordination, during stepping (Fig. 4C). Significant differences (Table 2) were observed between bipedal and quadrupedal distal angles at the trough (bipedal > quadrupedal), excursion of the distal angle (bipedal > quadrupedal), and phase relation between the two angles (bipedal > quadrupedal). The differences observed between bipedal and quadrupedal in angular kinematics could be inaccurate because of a couple of observations. The first cause might be a result of the elevation of the forelimbs (2 cm) on the resting platform during bipedal stepping changing the overall body angle. Alternatively, the great consistency of the data may explain some of the difference. For example, you can see in Table 2 that the phase relationship of bipedal at 2.5 km/h is 0.96 ± 0.02 and for quadrupedal it is 0.93 ± 0.02. Future studies should take this into consideration if comparing bipedal to quadrupedal stepping.

Interlimb coordination

Throughout all the tested quadrupedal walking speeds, animals displayed a lateral footfall sequence of RH, RF, LH, and LF (Fig. 7), consistent with a walking gait in which initiation of hindlimb swing (limb lift) is followed by swing initiation (lifting) of the ipsilateral forelimb.[79,92,93] During stepping, an average $50.4 \pm 2.74\%$ for homologous coupling was observed (Fig.7), as well as $28.5 \pm 3.59\%$ diagonal and $77.7 \pm 3.8\%$ homolateral couplings observed, in the hindlimbs at all speeds (Table 2). There were no significant differences among coupling measures between any of the speeds tested, or in homologous hindlimb coupling between bipedal and quadrupedal stepping. Mean diagonal coupling (mean lag time; Fig. 3) was 0.008 ± 0.005 sec (each frame is 0.00833 sec) at 2.5 km/h and was unchanged over all speeds tested. Figure 8 shows polar plots of the coupling measures for every step cycle for every animal. These plots show that at the speeds 1.0, 1.5, and 3.5 km/h, there is a greater variability than at the speeds 2.0, 2.5, and 3.0 km/h. This follows previously published data and demonstrates that you increase the consistency of stepping by choosing a speed within the range of 2.0 to 3.0 km/h.[49] The mean lag time at 2.5 km/h also shows consistency (low variability), in that the lag time of the first step remained relatively unchanged throughout the trial.

Discussion

In this study, we established the methodology for conducting treadmill-based kinematic testing in the healthy YMP and, in a series of 12 animals, have quantified effects of treadmill speed and differences between bipedal and quadrupedal locomotion. Bipedal and quadrupedal kinematic parameters of the pig were easily obtainable at multiple speeds on the treadmill using digital video capture and established kinematic analyses. Importantly, with the approaches used, no differences in key kinematic parameters of hindlimb stepping were identified between bipedal and quadrupedal locomotion. This suggests that the treadmill approach used was effective in recruiting primarily the spinal circuitry responsible for the basic stepping patterns as has been shown in cats.[22,61,64,68,71,74,76,94,95] The results demonstrate relative ease of training pigs to perform bipedal or quadrupedal stepping on a treadmill as an excellent model to test spinal circuitry responses to rehabilitative protocols with translational relevance similar to those used in the NeuroRecovery Networks® (NRN; The Reeve Foundation) locomotor training paradigms.[96] Both bipedal and quadrupedal training modes can be useful in injured animals to decipher intraspinal circuitry and impact of descending inputs.[44]

Step cycle summary and effects of speed

In rats and cats, an increase in treadmill speed from 7 to 15 cm/s (rats) and from 0.3 to 1.0 m/s (cats) was accompanied by shortening of stance durations and increases in stride distances with no changes in hindlimb swing durations.[18,21,44,97–99] These findings also have been observed in dogs[100] and chimpanzees.[81] Similarly, we observed that stride and stance durations decreased with increasing speed whereas the swing durations were not significantly affected. Whereas gait measures were more stable between 2.0 and 3.0 km/h (0.56–0.83 m/s), the stride distance began to elongate at 3.5 km/h (0.97 m/s), possibly indicating an impending to gait transition. We tested a single pig up to 5.5 km/h (unpublished data); whereas the pattern was still a walking pattern, a shift to a diagonal gait pattern was observed in which the contralateral forelimb follows the hindlimb.[40] This supports the speculation of an approaching gait transition at 3.5 km/h. The variability of stepping was higher at the lower speeds, and the animals reached a greater consistency ~2.0–3.0 km/h. This also is illustrated by the polar plots, which show greater spread of the interlimb phase relationships at speeds 1.0, 1.5, and 3.5 km/h compared to between 2.0 and 2.5 km/h (Fig. 4). Based on these results a speed of 2.5 km/h (0.7 m/s) is recommended for preclinical studies.

The variance in kinematic features observed at the lower gait speeds tested suggests that there is limited value in capturing gait performance at <2 km/h in the YMP as a baseline for comparisons with models in which gait is disrupted. Similarly, the higher speed tested (3.5 km/h) also may have limited value because of its proximity to a gait change. However, faster speeds (>3.5 km/h) may be valuable in testing an animal's ability to make speed-related transitions across gaits. The ability to transition reflects the integrity of underlying neural mechanisms, which support interlimb coordination involved in different gait patterns (e.g., walk, trot, and gallop in quadrupeds).[79,99,101–103]

Training paradigms involving all four limbs have been used to enhance locomotor recovery after SCI.[92,101,102] The general idea has been that recruitment of networks above the injury that communicate with those below the injury area may help with ambulatory recovery after injury.[103] Several studies reported differences in kinematics of bipedal versus quadrupedal treadmill walking.[79] In chimpanzees and macaques, a bipedal gait was associated with smaller step length, decreased step cycle duration, and increased duty factor.[79,81] In our study, we found no difference between quadrupedal and bipedal gait parameters at any speed. The percent stance or duty factor decreased with increasing speed and was greater (although not statistically significant) for bipedal at the higher speeds. These differences in bipedal versus quadrupedal treadmill kinematics between pigs and primates are not surprising given that the pig is a wholly quadrupedal animal. Its kinematics are

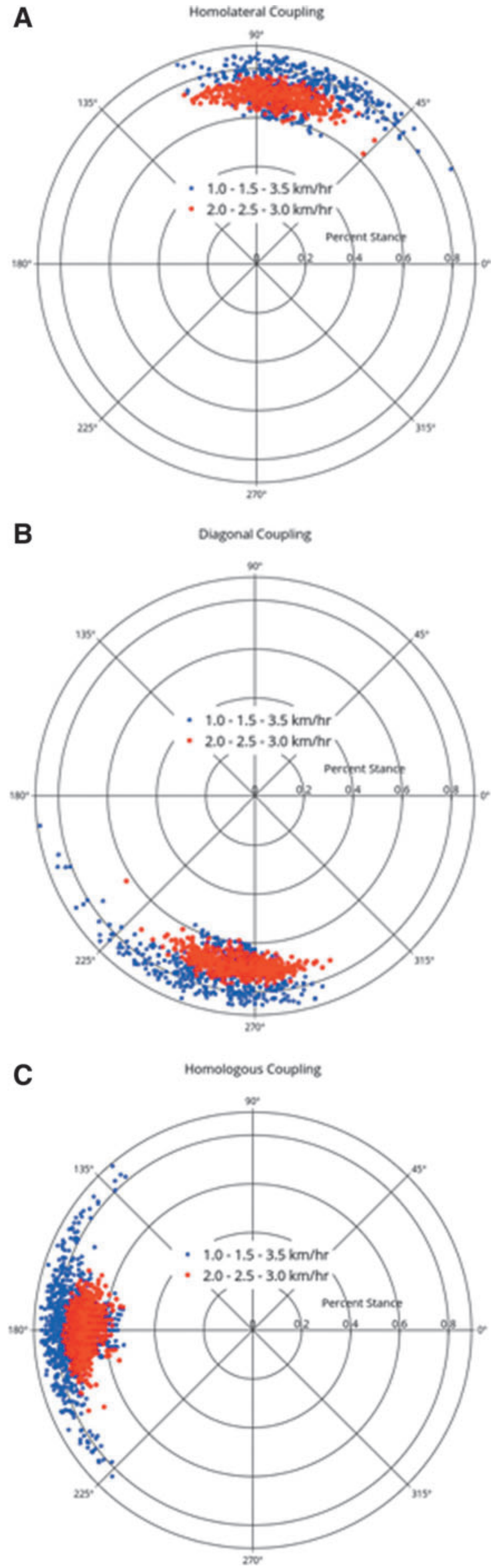

FIG. 8. Polar plots illustrating the coupling patterns of (**A**) diagonal, (**B**) homolateral, and (**C**) homologous hindlimb locomotion. Diagonal coupling shows the relationship of the hindlimb to its contralateral forelimb. Homolateral coupling shows the relationship between the hindlimb to its ipsilateral forelimb. Homologous coupling shows the relationship of the two hindlimbs to one another. In all three, there is a clear pattern of greater spread in 1.0-, 1.5-, and 3.5-km/h data (blue) compared to the tighter responses observed in the 2.0-, 2.5-, and 3.0-km/h data (red).

more similar to the cat, which showed similar indifferences between bipedal and quadrupedal gait.[82,87,104,105]

Overall, the results demonstrate that multiple hindlimb gait features are consistent across bipedal and quadrupedal stepping on a treadmill in the YMP. Inclusion of both bipedal and quadrupedal locomotion in future studies can help decipher intraspinal circuitry and impact of descending inputs. The angular kinematics tested in the present study were limited to two non-traditional angles not used in cats, primates, or humans. Therefore, we cannot rule out differences relative to more traditional angular kinematic measures used previously in those species.

Kinematics

Treadmill speed had no significant effect on the peaks, troughs, or excursions of the proximal and distal angles. This produced very similar angle-angle plots (cyclograms), which could be used to quantify differences post-injury by using elliptical Fourier analysis or a similar approach. These cyclograms also are a very informative graphic that can be used to depict recovery of range of motion across the joints, or overall limb movement. With the distal angle, we were able to identify the key step cycle parameters of initial contact, lift off, and yield. Yield, which involves the knee, is very important because it shows that even though we are not marking the knee, we are still able to identify loading of the limb.[93,106] Yield is an important part of a stable gait because it smooths out vertical movement, and it could be lost or diminished with spinal injury, resulting in poorer weight support and/or inappropriate stiffness of the limb resulting in disruption of stepping.

As with all the gait data, the angle kinematics were very consistent across all animals with little interanimal variability. The angles were so consistent that even a 6-degree mean difference between the bipedal distal angle trough and the quadrupedal distal angle trough was significant. The angle consistency may or may not be related to the single or multiple joints it encompasses. The high degree of consistency may be attributable to the reproducibility of key gait features and the 3 weeks of daily training the pigs received. Overall, the consistency of angle data support reproducibility because not all animals were recorded on the same day, and the range in animal size was 10 kg. Although the proximal and distal angles used here differ from more traditional angular kinematic measures, they are much easier to obtain and appear to be a good alternative to traditional four-segment, three-angle kinematics where the whole limb movement cannot be described by a single 2D angle-angle plot.

If the peak, trough, and angle excursions for bipedal movement are to be compared to those for quadrupedal movement, a normalization must be done to account for the change in body angle caused by the forelimb platform. These differences were attributed to the change in overall body angle of the pig caused by the increased elevation of the forelimb platform.

Intra- and interlimb coordination

In order to identify measures of coordination that could be used in future longitudinal studies, we quantified homologous, homolateral, and diagonal coupling parameters used in earlier studies in rodents and cats.[17,60,62,64,68,107] These measures have been used in many longitudinal kinematic studies in SCI animals[17,38,60,61,66,67,107]; for example, the homolateral coupling is perturbed by cord hemisections.[73] The homolateral coupling between hindlimbs and forelimbs ranged between 76% and 80% for all speeds, and the diagonal couplings ranged between 26% and 31%, which are similar to those reported in cats.[21,64] Diagonal interlimb coordination also was evaluated using the mean diagonal coupling (MDC) parameter described by Hamilton and colleagues.[40] In agreement, we observed that the MDC value was nearly zero at all speeds tested. The MDC has been shown to be sensitive to SCI-induced changes in interlimb coordination without being affected by abdominal support bands that are used to maintain normal posture and optimization of stepping in dogs.[40] Although the amount of diagonal coupling may vary among individual animals, the MDC appears to be less variable and has been proposed as a good parameter for canine clinical trials.[12,29,82,83] In addition to the interlimb couplings, the MDC is a parameter suitable for tracking outcome in porcine clinical trials.

Applications to study of kinematics in injured pigs

Utilization of the methods proposed here does require some weight-bearing capacity in the injured pig. In the original description of the porcine thoracic injury model, the 20-cm height drop with 5-min compression with a 100-g weight was recommended for testing of putative interventions.[23] This leads to a severe injury without weight-bearing capacity and limited spontaneous motor recovery (maximum PTIBS of 3–4). In animals with such severe injuries and insufficient spontaneous neurological recovery to allow sufficient weight-bearing capacity, varying degrees of body weight support may be necessary in order to assess gait kinematics on the treadmill. Many feline studies have demonstrated the ability to recover weight support after severe SCI or complete spinalization. Further, step training on the treadmill has been used to significantly improve walking in both the treadmill and overground environments.[59,66,69,108–111] Early preliminary data from ongoing studies in our laboratory show that pigs with moderate SCIs (10-cm height drop with 5-min compression) do recover some overground walking capacity, suggesting the feasibility of capturing treadmill-based gait in this group. These studies are being pursued as we work toward establishing a clinically relevant porcine SCI model.

In the more severely injured pig, however, a special harness can be designed and used for weight support. Indeed, in a pre-clinical study evaluating efficacy of magnesium chloride within polyethylene glycol formulation on recovery after SCI, Streijger and colleagues used a harness to provide weight support. This allowed collection of kinematic data while stepping on the treadmill in 3 of 6 pigs who had undergone 20-cm severe injuries.[35] The kinematic data analysis was possible with pigs that achieved a PTIBS score of 4, but not those with lower scores. Parameters measured included swing and stance durations and vertical and horizontal displacements of the hock and fetlock. Our study provides an expanded set of kinematic parameters, which include limb angles and measurements of interlimb coordination.

To date, the effects of training and gait rehabilitation approaches have not been tested in the porcine model. As an emerging model for SCI, it will be critical to assess the responsiveness of the injured pig to existing and evolving therapies, including locomotor training and epidural stimulation that have been shown to enhance motor recovery in other experimental species and humans. It is anticipated that these treatments, as in other species, will enhance weight support and allow gait assessment using a motorized treadmill in the pig. The results provided here in the normal YMP begin to establish a baseline for future study of kinematics across a range of SCI magnitudes in pigs. Further, they also provide a baseline for other existing and evolving neurological injury models in the pig, including stroke and traumatic brain injury.[112–114] Such animals showed sufficient weight bearing in recent reports.[112,114] Treadmill-based gait assessment has multiple advantages. It allows easy testing across gait speeds, permits assessment of both bipedal and quadrupedal forms of locomotion, is well suited to use of a body-weight support system, and permits rapid collection of a number of contiguous steps.

Limitations

The main limitation of our report is the use of proximal and distal angles not traditionally used in cat or human literature. A second limitation has been in the use of km/h attributed to pre-programming of our treadmill speeds in km/h whereas most cat literature uses m/s. The speeds used here—1.0 km/h (0.28 m/s) through 3.5 km/h (1 m/s)—are similar to previously used speeds (0.1–1.0 m/s) in cat kinematic studies.[18,21,56,57] A third limitation is the use of female pigs only. Performing these experiments on female animals exclusively facilitates post-SCI bladder care and urodynamic studies, given that urinary catheters cannot be placed into the bladder retrograde with the urethra of male pigs because of the urogenital anatomy.

Conclusion

We provided here treadmill-based kinematic data for healthy YMPs and quantified effects of treadmill speed and differences between bipedal and quadrupedal locomotion. The interlimb couplings—G-T-M distal angle and C-G-T proximal angles—and MDC are useful outcome variables that can be used to track outcomes in porcine studies and clinical trials in addition to the PTIBS used to assess overground gait. A speed of 2.5 km/h on the treadmill is recommended for pre-clinical studies. Future studies will focus on how these parameters are altered after SCI and examine correlations between these treadmill-based parameters and PTIBS scores.

Acknowledgments

We thank Drs. Alain Frigon and Serge Rossignol for their reviews and comments.

Funding Information

Research reported in this publication was supported by the Helmsley Foundation grant no. 2016PG-MED005, Department of Defense grant no. W81XWH-18-1-0117, Kentucky Spinal Cord Injury Center, The Veterans Affairs Rehabilitation, Research and Development RCSB92495, Ole A., Mabel Wise & Wilma Wise Nelson Endowment, the Rebecca F. Hammond Endowment, and the Craig F. Neilsen Foundation grant no. 546123.

Author Disclosure Statement

No competing financial interests exist.

Supplementary Material

Supplementary Data

References

1. National Spinal Cord Injury Statistical Center. Spinal Cord Injury: Facts and Figures at a Glance. 2019. https://www.nscisc.uab.edu/Public/Facts%20and%20Figures%202019%20-%20Final.pdf. Last accessed July 9, 2020.
2. Fehlings, M.G., Tetreault, L.A., Wilson, J.R., Aarabi, B., Anderson, P., Arnold, P.M., Brodke, D.S., Burns, A.S., Chiba, K., Dettori, J.R., Furlan, J.C., Hawryluk, G., Holly, L.T., Howley, S., Jeji, T., Kalsi-Ryan, S., Kotter, M., Kurpad, S., Marino, R.J., Martin, A.R., Massicotte, E., Merli, G., Middleton, J.W., Nakashima, H., Nagoshi, N., Palmieri, K., Singh, A., Skelly, A.C., Tsai, E.C., Vaccaro, A., Yee, A., and Harrop, J.S. (2017). A clinical practice guideline for the management of patients with acute spinal cord injury and central cord syndrome: recommendations on the timing (</=24 hours versus >24 hours) of decompressive surgery. Global Spine J. 7, 3 Suppl., 195S–202S.
3. Readdy, W.J., Chan, A.K., Matijakovich, D.J., and Dhall, S.D. (2015). A review and update on the guidelines for the acute non-operative management of cervical spinal cord injury. J. Neurosurg. Sci. 59, 119–128.
4. Yue, J.K., Chan, A.K., Winkler, E.A., Upadhyayula, P.S., Readdy, W.J., and Dhall, S.S. (2016). A review and update on the guidelines for the acute management of cervical spinal cord injury—part II. J. Neurosurg. Sci. 60, 367–384.
5. Nardone, R., Florea, C., Holler, Y., Brigo, F., Versace, V., Lochner, P., Golaszewski, S., and Trinka, E. (2017). Rodent, large animal and non-human primate models of spinal cord injury. Zoology (Jena) 123, 101–114.
6. Ma, Z., Zhang, Y.P., Liu, W., Yan, G., Li, Y., Shields, L.B.E., Walker, M., Chen, K., Huang, W., Kong, M., Lu, Y., Brommer, B., Chen, X., Xu, X.M., and Shields, C.B. (2016). A controlled spinal cord contusion for the rhesus macaque monkey. Exp. Neurol. 279, 261–273.
7. Courtine, G., Bunge, M.B., Fawcett, J.W., Grossman, R.G., Kaas, J.H., Lemon, R., Maier, I., Martin, J., Nudo, R.J., Ramon-Cueto, A., Rouiller, E.M., Schnell, L., Wannier, T., Schwab, M.E., and Edgerton, V.R. (2007). Can experiments in nonhuman primates expedite the translation of treatments for spinal cord injury in humans? Nat. Med. 13, 561–566.
8. Hurd, C., Weishaupt, N., and Fouad, K. (2013). Anatomical correlates of recovery in single pellet reaching in spinal cord injured rats. Exp. Neurol. 247, 605–614.
9. Sterr, A., Shen, S., Szameitat, A.J., and Herron, K.A. (2010). The role of corticospinal tract damage in chronic motor recovery and neurorehabilitation: a pilot study. Neurorehabil. Neural Repair 24, 413–419.
10. Anderson, K.D., Sharp, K.G., and Steward, O. (2009). Bilateral cervical contusion spinal cord injury in rats. Exp. Neurol. 220, 9–22.
11. Kwon, B.K., Streijger, F., Hill, C.E., Anderson, A.J., Bacon, M., Beattie, M.S., Blesch, A., Bradbury, E.J., Brown, A., Bresnahan, J.C., Case, C.C., Colburn, R.W., David, S., Fawcett, J.W., Ferguson, A.R., Fischer, I., Floyd, C.L., Gensel, J.C., Houle, J.D., Jakeman, L.B., Jeffery, N.D., Jones, L.A., Kleitman, N., Kocsis, J., Lu, P., Magnuson, D.S., Marsala, M., Moore, S.W., Mothe, A.J., Oudega, M., Plant, G.W., Rabchevsky, A.S., Schwab, J.M., Silver, J., Steward, O., Xu, X.M., Guest, J.D., and Tetzlaff, W. (2015). Large animal and primate models of spinal cord injury for the testing of novel therapies. Exp. Neurol. 269, 154–168.
12. Jeffery, N.D., Hamilton, L., and Granger, N. (2011). Designing clinical trials in canine spinal cord injury as a model to translate successful laboratory interventions into clinical practice. Vet. Rec. 168, 102–107.
13. Nadeau, S., Jacquemin, G., Fournier, C., Lamarre, Y., and Rossignol, S. (2010). Spontaneous motor rhythms of the back and legs in a patient with a complete spinal cord transection. Neurorehabil. Neural Repair 24, 377–383.
14. Martinez, M., and Rossignol, S. (2013). A dual spinal cord lesion paradigm to study spinal locomotor plasticity in the cat. Ann. N. Y. Acad. Sci. 1279, 127–134.
15. Martinez, M., Tuznik, M., Delivet-Mongrain, H., and Rossignol, S. (2013). Emergence of deletions during treadmill locomotion as a function of supraspinal and sensory inputs. J. Neurosci. 33, 11599–11605.
16. Martinez, M., and Rossignol, S. (2011). Changes in CNS structures after spinal cord lesions implications for BMI. Prog. Brain Res. 194, 191–202.
17. Martinez, M., Delivet-Mongrain, H., Leblond, H., and Rossignol, S. (2011). Recovery of hindlimb locomotion after incomplete spinal cord injury in the cat involves spontaneous compensatory changes within the spinal locomotor circuitry. J. Neurophysiol. 106, 1969–1984.
18. Harnie, J., Cote-Sarrazin, C., Hurteau, M.F., Desrochers, E., Doelman, A., Amhis, N., and Frigon, A. (2018). The modulation of locomotor speed is maintained following partial denervation of ankle extensors in spinal cats. J. Neurophysiol. 120, 1274–1285.
19. Grillner, S., and Rossignol, S. (1978). On the initiation of the swing phase of locomotion in chronic spinal cats. Brain Res. 146, 269–277.

20. Gossard, J.P., Delivet-Mongrain, H., Martinez, M., Kundu, A., Escalona, M., and Rossignol, S. (2015). Plastic changes in lumbar locomotor networks after a partial spinal cord injury in cats. J. Neurosci. 35, 9446–9455.
21. Frigon, A., D'Angelo, G., Thibaudier, Y., Hurteau, M.F., Telonio, A., Kuczynski, V., and Dambreville, C. (2014). Speed-dependent modulation of phase variations on a step-by-step basis and its impact on the consistency of interlimb coordination during quadrupedal locomotion in intact adult cats. J. Neurophysiol. 111, 1885–1902.
22. Frigon, A., and Rossignol, S. (2008). Adaptive changes of the locomotor pattern and cutaneous reflexes during locomotion studied in the same cats before and after spinalization. J. Physiol. 586, 2927–2945.
23. Lee, J.H., Jones, C.F., Okon, E.B., Anderson, L., Tigchelaar, S., Kooner, P., Godbey, T., Chua, B., Gray, G., Hildebrandt, R., Cripton, P., Tetzlaff, W., and Kwon, B.K. (2013). A novel porcine model of traumatic thoracic spinal cord injury. J. Neurotrauma 30, 142–159.
24. Schomberg, D.T., Miranpuri, G.S., Chopra, A., Patel, K., Meudt, J.J., Tellez, A., Resnick, D.K., and Shanmuganayagam, D. (2017). Translational relevance of swine models of spinal cord injury. J. Neurotrauma 34, 541–551.
25. Kwon, B.K., Stammers, A.M., Belanger, L.M., Bernardo, A., Chan, D., Bishop, C.M., Slobogean, G.P., Zhang, H., Umedaly, H., Giffin, M., Street, J., Boyd, M.C., Paquette, S.J., Fisher, C.G., and Dvorak, M.F. (2010). Cerebrospinal fluid inflammatory cytokines and biomarkers of injury severity in acute human spinal cord injury. J. Neurotrauma 27, 669–682.
26. Squair, J.W., Belanger, L.M., Tsang, A., Ritchie, L., Mac-Thiong, J.M., Parent, S., Christie, S., Bailey, C., Dhall, S., Street, J., Ailon, T., Paquette, S., Dea, N., Fisher, C.G., Dvorak, M.F., West, C.R., and Kwon, B.K. (2017). Spinal cord perfusion pressure predicts neurologic recovery in acute spinal cord injury. Neurology 89, 1660–1667.
27. Streijger, F., So, K., Manouchehri, N., Tigchelaar, S., Lee, J.H.T., Okon, E.B., Shortt, K., Kim, S.E., McInnes, K., Cripton, P., and Kwon, B.K. (2017). Changes in pressure, hemodynamics, and metabolism within the spinal cord during the first 7 days after injury using a porcine model. J. Neurotrauma 34, 3336–3350.
28. Tigchelaar, S., Gupta, R., Shannon, C.P., Streijger, F., Sinha, S., Flibotte, S., Rizzuto, M.A., Street, J., Paquette, S., Ailon, T., Charest-Morin, R., Dea, N., Fisher, C., Dvorak, M.F., Dhall, S., Mac-Thiong, J.M., Parent, S., Bailey, C., Christie, S., Van Keuren-Jensen, K., Nislow, C., and Kwon, B.K. (2019). MicroRNA biomarkers in cerebrospinal fluid and serum reflect injury severity in human acute traumatic spinal cord injury. J. Neurotrauma 36, 2358–2371.
29. Hachmann, J.T., Jeong, J.H., Grahn, P.J., Mallory, G.W., Evertz, L.Q., Bieber, A.J., Lobel, D.A., Bennet, K.E., Lee, K.H., and Lujan, J.L. (2013). Large animal model for development of functional restoration paradigms using epidural and intraspinal stimulation. PLoS One 8, e81443.
30. Cuellar, C.A., Mendez, A.A., Islam, R., Calvert, J.S., Grahn, P.J., Knudsen, B., Pham, T., Lee, K.H., and Lavrov, I.A. (2017). The role of functional neuroanatomy of the lumbar spinal cord in effect of epidural stimulation. Front. Neuroanat. 11, 82.
31. Guiho, T., Azevedo-Coste, C., Andreu, D., Delleci, C., Bauchet, L., Vignes, J.R., and Guiraud, D. (2018). Functional selectivity of lumbosacral stimulation: methodological approach and pilot study to assess visceral function in pigs. IEEE Trans. Neural Syst. Rehabil. Eng. 26, 2165–2178.
32. Guiho, T., Delleci, C., Azevedo-Coste, C., Fattal, C., Guiraud, D., Vignes, J.R., and Bauchet, L. (2018). Impact of direct epispinal stimulation on bladder and bowel functions in pigs: a feasibility study. Neurourol. Urodyn. 37, 138–147.
33. Dalkilic, T., Fallah, N., Noonan, V.K., Salimi Elizei, S., Dong, K., Belanger, L., Ritchie, L., Tsang, A., Bourassa-Moreau, E., Heran, M.K.S., Paquette, S.J., Ailon, T., Dea, N., Street, J., Fisher, C.G., Dvorak, M.F., and Kwon, B.K. (2018). Predicting injury severity and neurological recovery after acute cervical spinal cord injury: a comparison of cerebrospinal fluid and magnetic resonance imaging biomarkers. J. Neurotrauma 35, 435–445.
34. Streijger, F., Lee, J.H., Chak, J., Dressler, D., Manouchehri, N., Okon, E.B., Anderson, L.M., Melnyk, A.D., Cripton, P.A., and Kwon, B.K. (2015). The effect of whole-body resonance vibration in a porcine model of spinal cord injury. J. Neurotrauma 32, 908–921.
35. Streijger, F., Lee, J.H., Manouchehri, N., Okon, E.B., Tigchelaar, S., Anderson, L.M., Dekaban, G.A., Rudko, D.A., Menon, R.S., Iaci, J.F., Button, D.C., Vecchione, A.M., Konovalov, A., Sarmiere, P.D., Ung, C., Caggiano, A.O., and Kwon, B.K. (2016). The evaluation of magnesium chloride within a polyethylene glycol formulation in a porcine model of acute spinal cord injury. J. Neurotrauma 33, 2202–2216.
36. Basso, D.M., Beattie, M.S., and Bresnahan, J.C. (1995). A sensitive and reliable locomotor rating scale for open field testing in rats. J. Neurotrauma 12, 1–21.
37. Diogo, C.C., da Costa, L.M., Pereira, J.E., Filipe, V., Couto, P.A., Geuna, S., Armada-da-Silva, P.A., Mauricio, A.C., and Varejao, A.S.P. (2019). Kinematic and kinetic gait analysis to evaluate functional recovery in thoracic spinal cord injured rats. Neurosci. Biobehav. Rev. 98, 18–28.
38. Alluin, O., Karimi-Abdolrezaee, S., Delivet-Mongrain, H., Leblond, H., Fehlings, M.G., and Rossignol, S. (2011). Kinematic study of locomotor recovery after spinal cord clip compression injury in rats. J. Neurotrauma 28, 1963–1981.
39. Leblond, H., L'Esperance, M., Orsal, D., and Rossignol, S. (2003). Treadmill locomotion in the intact and spinal mouse. J. Neurosci. 23, 11411–11419.
40. Hamilton, L., Franklin, R.J., and Jeffery, N.D. (2007). Development of a universal measure of quadrupedal forelimb-hindlimb coordination using digital motion capture and computerised analysis. BMC Neurosci. 8, 77.
41. Hamilton, L., Franklin, R.J., and Jeffery, N.D. (2008). Quantification of deficits in lateral paw positioning after spinal cord injury in dogs. BMC Vet. Res. 4, 47.
42. Safayi, S., Jeffery, N.D., Shivapour, S.K., Zamanighomi, M., Zylstra, T.J., Bratsch-Prince, J., Wilson, S., Reddy, C.G., Fredericks, D.C., Gillies, G.T., and Howard, M.A. III. (2015). Kinematic analysis of the gait of adult sheep during treadmill locomotion: parameter values, allowable total error, and potential for use in evaluating spinal cord injury. J. Neurol. Sci. 358, 107–112.
43. Safayi, S., Miller, J.W., Wilson, S., Shivapour, S.K., Oelfke, T.F., Ford, A.L., Klarmann Staudt, A., Abode-Iyamah, K., Reddy, C.G., Jeffery, N.D., Fredericks, D.C., Gillies, G.T., and Howard, M.A. III. (2016). Treadmill measures of ambulation rates in ovine models of spinal cord injury and neuropathic pain. J. Med. Eng. Technol. 40, 72–79.
44. Goldberger, M.E., Bregman, B.S., Vierck, C.J., and Brown, M. (1990). Criteria for assessing recovery of function after spinal cord injury: behavioral methods. Exp. Neurol. 107, 113–117.
45. Awai, L., and Curt, A. (2014). Intralimb coordination as a sensitive indicator of motor-control impairment after spinal cord injury. Front. Hum. Neurosci. 8, 148.
46. Awai, L., Bolliger, M., Ferguson, A.R., Courtine, G., and Curt, A. (2016). Influence of spinal cord integrity on gait control in human spinal cord injury. Neurorehabil. Neural Repair 30, 562–572.
47. Awai, L., and Curt, A. (2016). Locomotor recovery in spinal cord injury: insights beyond walking speed and distance. J. Neurotrauma 33, 1428–1435.
48. Easthope, C.S., Traini, L.R., Awai, L., Franz, M., Rauter, G., Curt, A., and Bolliger, M. (2018). Overground walking patterns after chronic incomplete spinal cord injury show distinct response patterns to unloading. J. Neuroeng. Rehabil. 15, 102.
49. Malik, R.N., Eginyan, G., Lynn, A.K., and Lam, T. (2019). Improvements in skilled walking associated with kinematic adaptations in people with spinal cord injury. J. Neuroeng. Rehabil. 16, 107.
50. Hansen, C.N., Linklater, W., Santiago, R., Fisher, L.C., Moran, S., Buford, J.A., and Michele Basso, D. (2012). Characterization of recovered walking patterns and motor control after contusive spinal cord injury in rats. Brain Behav. 2, 541–552.
51. Antri, M., Mouffle, C., Orsal, D., and Barthe, J.Y. (2003). 5-HT1A receptors are involved in short- and long-term processes responsible for 5-HT-induced locomotor function recovery in chronic spinal rat. Eur. J. Neurosci. 18, 1963–1972.
52. Antri, M., Orsal, D., and Barthe, J.Y. (2002). Locomotor recovery in the chronic spinal rat: effects of long-term treatment with a 5-HT2 agonist. Eur. J. Neurosci. 16, 467–476.
53. Stavrakakis, S., Guy, J.H., Warlow, O.M.E., Johnson, G.R., and Edwards, S.A. (2014). Intra-operator repeatability of skin marker derived segment measures and gait kinematics in healthy pigs. Biosyst. Eng. 118, 1–6.
54. Stavrakakis, S., Guy, J.H., Warlow, O.M., Johnson, G.R., and Edwards, S.A. (2014). Longitudinal gait development and variability of growing pigs reared on three different floor types. Animal 8, 338–346.

55. Stavrakakis, S., Guy, J.H., Syranidis, I., Johnson, G.R., and Edwards, S.A. (2015). Pre-clinical and clinical walking kinematics in female breeding pigs with lameness: a nested case-control cohort study. Vet. J. 205, 38–43.
56. Dambreville, C., Labarre, A., Thibaudier, Y., Hurteau, M.F., and Frigon, A. (2015). The spinal control of locomotion and step-to-step variability in left-right symmetry from slow to moderate speeds. J. Neurophysiol. 114, 1119–1128.
57. D'Angelo, G., Thibaudier, Y., Telonio, A., Hurteau, M.F., Kuczynski, V., Dambreville, C., and Frigon, A. (2014). Modulation of phase durations, phase variations, and temporal coordination of the four limbs during quadrupedal split-belt locomotion in intact adult cats. J. Neurophysiol. 112, 1825–1837.
58. Thibaudier, Y., Hurteau, M.F., Dambreville, C., Chraibi, A., Goetz, L., and Frigon, A. (2017). Interlimb coordination during tied-belt and transverse split-belt locomotion before and after an incomplete spinal cord injury. J. Neurotrauma 34, 1751–1765.
59. Barbeau, H., and Rossignol, S. (1987). Recovery of locomotion after chronic spinalization in the adult cat. Brain Res. 412, 84–95.
60. Barriere, G., Frigon, A., Leblond, H., Provencher, J., and Rossignol, S. (2010). Dual spinal lesion paradigm in the cat: evolution of the kinematic locomotor pattern. J. Neurophysiol. 104, 1119–1133.
61. Belanger, M., Drew, T., Provencher, J., and Rossignol, S. (1996). A comparison of treadmill locomotion in adult cats before and after spinal transection. J. Neurophysiol. 76, 471–491.
62. Brustein, E., and Rossignol, S. (1998). Recovery of locomotion after ventral and ventrolateral spinal lesions in the cat. I. Deficits and adaptive mechanisms. J. Neurophysiol. 80, 1245–1267.
63. Cohen-Adad, J., Martinez, M., Delivet-Mongrain, H., and Rossignol, S. (2014). Recovery of locomotion after partial spinal cord lesions in cats: assessment using behavioral, electrophysiological and imaging techniques. Acta Neurobiol. Exp. (Wars.) 74, 142–157.
64. Escalona, M., Delivet-Mongrain, H., Kundu, A., Gossard, J.P. and Rossignol, S. (2017). Ladder treadmill: a method to assess locomotion in cats with an intact or lesioned spinal cord. J. Neurosci. 37, 5429–5446.
65. Forssberg, H., Grillner, S., Halbertsma, J., and Rossignol, S. (1980). The locomotion of the low spinal cat. II. Interlimb coordination. Acta Physiol. Scand. 108, 283–295.
66. Martinez, M., Delivet-Mongrain, H., Leblond, H., and Rossignol, S. (2012). Effect of locomotor training in completely spinalized cats previously submitted to a spinal hemisection. J. Neurosci. 32, 10961–10970.
67. Martinez, M., Delivet-Mongrain, H., Leblond, H., and Rossignol, S. (2012). Incomplete spinal cord injury promotes durable functional changes within the spinal locomotor circuitry. J. Neurophysiol. 108, 124–134.
68. Martinez, M., Delivet-Mongrain, H., and Rossignol, S. (2013). Treadmill training promotes spinal changes leading to locomotor recovery after partial spinal cord injury in cats. J. Neurophysiol. 109, 2909–2922.
69. Rossignol, S., Chau, C., Brustein, E., Belanger, M., Barbeau, H., and Drew, T. (1996). Locomotor capacities after complete and partial lesions of the spinal cord. Acta Neurobiol. Exp. (Wars.) 56, 449–463.
70. Rossignol, S., Chau, C., Brustein, E., Giroux, N., Bouyer, L., Barbeau, H., and Reader, T.A. (1998). Pharmacological activation and modulation of the central pattern generator for locomotion in the cat. Ann. N. Y. Acad. Sci. 860, 346–359.
71. Rossignol, S., Belanger, M., Chau, C., Giroux, N., Brustein, E., Bouyer, L., Grenier, C.-A., Drew, T., Barbeau, H., and Reader, T. (2000). The spinal cat, in: *Neurobiology of Spinal Cord Injury*. R.G. Kalb and S.M. Strittmatter (eds). Humana: Totowa, NJ, pps. 57–87.
72. Rossignol, S. (2006). Plasticity of connections underlying locomotor recovery after central and/or peripheral lesions in the adult mammals. Philos. Trans. R. Soc. Lond. B. Biol. Sci. 361, 1647–1671.
73. Rossignol, S., Barriere, G., Alluin, O., and Frigon, A. (2009). Re-expression of locomotor function after partial spinal cord injury. Physiology (Bethesda) 24, 127–139.
74. Rossignol, S., Frigon, A., Barriere, G., Martinez, M., Barthelemy, D., Bouyer, L., Belanger, M., Provencher, J., Chau, C., Brustein, E., Barbeau, H., Giroux, N., Marcoux, J., Langlet, C., and Alluin, O. (2011). Spinal plasticity in the recovery of locomotion. Prog. Brain Res. 188, 229–241.
75. Rossignol, S., and Frigon, A. (2011). Recovery of locomotion after spinal cord injury: some facts and mechanisms. Annu. Rev. Neurosci. 34, 413–440.
76. Rossignol, S., Martinez, M., Escalona, M., Kundu, A., Delivet-Mongrain, H., Alluin, O., and Gossard, J.P. (2015). The ''beneficial'' effects of locomotor training after various types of spinal lesions in cats and rats. Prog. Brain Res. 218, 173–198.
77. de Leon, R.D., Hodgson, J.A., Roy, R.R., and Edgerton, V.R. (1998). Locomotor capacity attributable to step training versus spontaneous recovery after spinalization in adult cats. J. Neurophysiol. 79, 1329–1340.
78. Berillon, G., Daver, G., D'Août, K., Nicolas, G., de la Villetanet, B., Multon, F., Digrandi, G., and Dubreuil, G. (2010). Bipedal versus quadrupedal hind limb and foot kinematics in a captive sample of *Papio anubis*: setup and preliminary results. Int. J. Primatol. 31, 159–180.
79. Higurashi, Y., Maier, M.A., Nakajima, K., Morita, K., Fujiki, S., Aoi, S., Mori, F., Murata, A., and Inase, M. (2019). Locomotor kinematics and EMG activity during quadrupedal versus bipedal gait in the Japanese macaque. J. Neurophysiol. 122, 398–412.
80. Howland, D.R., Bregman, B.S., and Goldberger, M.E. (1995). The development of quadrupedal locomotion in the kitten. Exp. Neurol. 135, 93–107.
81. Pontzer, H., Raichlen, D.A., and Rodman, P.S. (2014). Bipedal and quadrupedal locomotion in chimpanzees. J. Hum. Evol. 66, 64–82.
82. Zelenin, P.V., Deliagina, T.G., Orlovsky, G.N., Karayannidou, A., Dasgupta, N.M., Sirota, M.G., and Beloozerova, I.N. (2011). Contribution of different limb controllers to modulation of motor cortex neurons during locomotion. J. Neurosci. 31, 4636–4649.
83. Pryor, K. (1999). *Don't Shoot the Dog!: The New Art of Teaching and Training*. Bantam: New York.
84. Pryor, K. (2010). *Reaching the Animal Mind: Clicker Training and What It Teaches Us about All Animals*. Scribner: New York.
85. Zeltner, A. (2013). Handling, Dosing and Training of the Göttingen Minipig. https://pdfs.semanticscholar.org/eb57/98946bb29d80962202f37f770b07d1ae2c6c.pdf. Last accessed July 9, 2020.
86. Blye, R., Burke, R., James, C., Fitzgerald, A.L., and Cox, M.L. (2006). The use of operant conditioning of Göttingen minipigs for topical safety studies. American Association for Laboratory Animal Science Meeting Official Program: 153–154 (Abstract).
87. Hildebrand, M. (1976). Analysis of tetrapod gaits: general considerations and symmetrical gaits, in: *Neural Control of Locomotion*. R.M. Herman, S. Grillner, P.S.G. Stein, and D.G. Stuart (eds). Plenum: New York, pps. 203–236.
88. Barbeau, H., and Rossignol, S. (1987). Recovery of locomotion after chronic spinalization in the adult cat. Brain Res. 412, 84–95.
89. Magnuson, D.S., Smith, R.R., Brown, E.H., Enzmann, G., Angeli, C., Quesada, P.M., and Burke, D. (2009). Swimming as a model of task-specific locomotor retraining after spinal cord injury in the rat. Neurorehabil. Neural Repair 23, 535–545.
90. Thota, A., Carlson, S., and Jung, R. (2001). Recovery of locomotor function after treadmill training of incomplete spinal cord injured rats. Biomed. Sci. Instrum. 37, 63–67.
91. Kuerzi, J., Brown, E.H., Shum-Siu, A., Siu, A., Burke, D., Morehouse, J., Smith, R.R., and Magnuson, D.S. (2010). Task-specificity vs. ceiling effect: step-training in shallow water after spinal cord injury. Exp. Neurol. 224, 178–187.
92. Shah, P.K., Garcia-Alias, G., Choe, J., Gad, P., Gerasimenko, Y., Tillakaratne, N., Zhong, H., Roy, R.R., and Edgerton, V.R. (2013). Use of quadrupedal step training to re-engage spinal interneuronal networks and improve locomotor function after spinal cord injury. Brain 136, 3362–3377.
93. English, A.W., and Lennard, P.R. (1982). Interlimb coordination during stepping in the cat: in-phase stepping and gait transitions. Brain Res. 245, 353–364.
94. Grillner, S. (1973). Locomotion in the spinal cat, in: *Control of Posture and Locomotion. Advanced Behavioral Biology*. R.B. Stein, K.G. Pearson, R.S. Smith, and J.B. Redford (eds). Plenum: New York, pps. 515–535.
95. Belanger, M., Drew, T., and Rossignol, S. (1988). Spinal locomotion: a comparison of the kinematics and the electromyographic activity in the same animal before and after spinalization. Acta Biol. Hung. 39, 151–154.
96. Buehner, J.J., Forrest, G.F., Schmidt-Read, M., White, S., Tansey, K., and Basso, D.M. (2012). Relationship between ASIA examination and functional outcomes in the NeuroRecovery Network Locomotor Training Program. Arch. Phys. Med. Rehabil. 93, 1530–1540.

97. Beare, J.E., Morehouse, J.R., DeVries, W.H., Enzmann, G.U., Burke, D.A., Magnuson, D.S., and Whittemore, S.R. (2009). Gait analysis in normal and spinal contused mice using the TreadScan system. J. Neurotrauma 26, 2045–2056.
98. Herbin, M., Gasc, J.P., and Renous, S. (2004). Symmetrical and asymmetrical gaits in the mouse: patterns to increase velocity. J. Comp. Physiol. A Neuroethol. Sens. Neural Behav. Physiol. 190, 895–906.
99. Clarke, K.A., and Still, J. (1999). Gait analysis in the mouse. Physiol. Behav. 66, 723–729.
100. Maes, L.D., Herbin, M., Hackert, R., Bels, V.L., and Abourachid, A. (2008). Steady locomotion in dogs: temporal and associated spatial coordination patterns and the effect of speed. J. Exp. Biol. 211, 138–149.
101. Gumbel, J.H., Steadman, C.J., Hoey, R.F., Armstrong, J.E., Fell, J.D., Yang, C.B., Montgomery, L.R., and Hubscher, C.H. (2019). Activity-based training on a treadmill with spinal cord injured wistar rats. J. Vis. Exp. (143), e58983.
102. Hubscher, C.H., Montgomery, L.R., Fell, J.D., Armstrong, J.E., Poudyal, P., Herrity, A.N., and Harkema, S.J. (2016). Effects of exercise training on urinary tract function after spinal cord injury. Am. J. Physiol. Renal Physiol. 310, F1258–F1268.
103. Frigon, A. (2017). The neural control of interlimb coordination during mammalian locomotion. J. Neurophysiol. 117, 2224–2241.
104. Hildebrand, M. (1965). Symmetrical gaits of horses. Science 150, 701–708.
105. Hildebrand, M. (1989). The quadrupedal gaits of vertebrates. BioScience 39, 766–775.
106. English, A.W. (1978). An electromyographic analysis of forelimb muscles during overground stepping in the cat. J. Exp. Biol. 76, 105–122.
107. Jefferson, S.C., Tester, N.J., and Howland, D.R. (2011). Chondroitinase ABC promotes recovery of adaptive limb movements and enhances axonal growth caudal to a spinal hemisection. J. Neurosci. 31, 5710–5720.
108. Delivet-Mongrain, H., Dea, M., Gossard, J.-P., and Rossignol, S. (2020). Recovery of locomotion in cats after severe contusion of the low thoracic spinal cord. J. Neurophysiol. 123, 1504–1525.
109. De Leon, R.D., Hodgson, J.A., Roy, R.R., and Edgerton, V.R. (1998). Full weight-bearing hindlimb standing following stand training in the adult spinal cat. J. Neurophysiol. 80, 83–91.
110. Lovely, R.G., Gregor, R.J., Roy, R.R., and Edgerton, V.R. (1990). Weight-bearing hindlimb stepping in treadmill-exercised adult spinal cats. Brain Res. 514, 206–218.
111. Lovely, R.G., Gregor, R.J., Roy, R.R., and Edgerton, V.R. (1986). Effects of training on the recovery of full-weight-bearing stepping in the adult spinal cat. Exp. Neurol. 92, 421–435.
112. Baker, E.W., Kinder, H.A., Hutcheson, J.M., Duberstein, K.J.J., Platt, S.R., Howerth, E.W., and West, F.D. (2019). Controlled cortical impact severity results in graded cellular, tissue, and functional responses in a piglet traumatic brain injury model. J. Neurotrauma 36, 61–73.
113. Platt, S.R., Holmes, S.P., Howerth, E.W., Duberstein, K.J.J., Dove, C.R., Kinder, H.A., Wyatt, E.L., Linville, A.V., Lau, V.W., Stice, S.L., Hill, W.D., Hess, D.C., and West, F.D. (2014). Development and characterization of a Yucatan miniature biomedical pig permanent middle cerebral artery occlusion stroke model. Exp. Transl. Stroke Med. 6, 5.
114. Kaiser, E.E., Waters, E.S., Fagan, M.M., Scheulin, K.M., Platt, S.R., Jeon, J.H., Fang, X., Kinder, H.A., Shin, S.K., Duberstein, K.J., Park, H.J., and West, F.D. (2020). Characterization of tissue and functional deficits in a clinically translational pig model of acute ischemic stroke. Brain Res. 1736, 146778.

Address correspondence to:
Maxwell Boakye, MD, MPH, MBA, FAANS, FACS
Department of Neurosurgery
University of Louisville
220 Abraham Flexner Way, 15th Floor
Louisville, KY 40202
USA

E-mail: max.boakye@louisville.edu